Electronic Supplementary Material (ESI) for ChemComm.

Supporting Information for:

The Facile Realization of RGB Luminescence based on One Yellow Emissive Four-Coordinate Boron-Containing Material

Lu Wang, Kai Wang, Houyu Zhang, Chuanjun Jiao, Bo Zou*, Kaiqi Ye, Hongyu Zhang* and Yue Wang

General information

1,3-Diaryl-*β*-diketone and fluorobis(pentafluorophenyl)borane was synthesized according to the reported procedure. Other starting materials were common commercial grade and used as received. The solvents for syntheses were freshly distilled over appropriate drying reagents. All experiments were performed under a nitrogen atmosphere using standard Schlenk techniques. NMR spectra were recorded on a Bruker AVANCE 500 MHz spectrometer with tetramethylsilane as the internal standard. Mass spectra were recorded on a GC/MS mass spectrometer. Element analyses were performed on a FlashEA1112 spectrometer. UV-vis absorption spectra were recorded by a Shimadzu UV-2550 spectrophotometer. Melting points were determined on a Kofler hot-stage. The emission spectra of solutions were recorded by a ShimadzuRF-5301 PC spectrometer or a Maya2000 Pro CCD spectrometer. Differential scanning calorimetric (DSC) measurements were performed on a NETZSCH DSC204 instrument at a heating rate of 10 °C min^{-1} under nitrogen. Thermogravimetric analyses (TGA) were performed on a TAQ500 thermogravimeter at a heating rate of 10 °C min^{-1} under nitrogen. Powder X-ray diffraction data were collected at 298K on a Bruker SMART-CCD diffractometer. The absolute fluorescence quantum yields were measured on Edinburgh FLS920 using an integrating sphere. The fluorescence lifetimes were measured on Edinburgh FLS920 using a time-correlated single-photon (TCSPC) module.

Scheme S1 Synthetic procedure of boron compounds **1**.

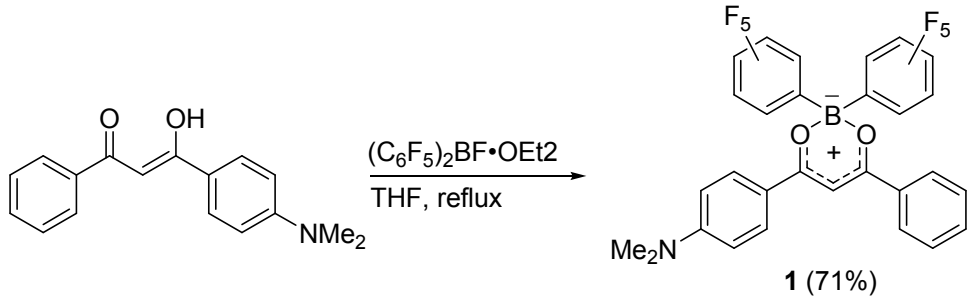

1 (71%)

Synthesis of boron compounds 1

$(C_6F_5)_2BF{\cdot}OEt_2$ (4.13 mmol) was added to a solution of (*Z*)-3-(4-(methylamino)phenyl)-3-hydroxyprop-2-en-1-one (3.75 mmol) in THF under nitrogen. The mixture was heated to reflux for 12 h. After cooling, the produced precipitates were filtered and recrystallized from CH_2Cl_2/MeOH 1:3 to yield the pure boron products.

Data of compound **1**. Yields: 71%. Mp: 248−250 °C. ^{1}H NMR ($CDCl_3$, 500 MHz, ppm): δ 8.10 (t, J = 10.0 Hz, 4 H), 7.62 (t, J = 5.0 Hz, 1 H), 7.52 (t, J = 10.0 Hz, 2 H), 6.96 (s, 1 H), 6.80 (d, J = 10.0 Hz, 2 H), 3.18 (s, 6 H). ^{13}C NMR ($CDCl_3$, 125 MHz, ppm): δ 180.63, 177.83, 155.41, 149.18, 147.25, 141.13, 139.14, 138.04, 136.09, 133.79, 133.11, 132.26, 128.94, 128.37, 111.52, 92.09, 40.17. MS m/z: 611.28 [M^+] (calcd: 611.11). Anal.Calcd (%) for $C_{29}H_{16}BF_{10}NO_2$: C, 56.98; H, 2.64; N, 2.29; Found: C, 57.16; H, 2.79; N, 2.34.

High-pressure experiments

The tiny crystal was placed in the hole(diameter: 200 mm) of a T301 steel gasket, A silicone oil was used as a pressure transmit medium (PTM). In situ steady-state PL measurement under high pressure were performed on a Ocean Optics QE65000 spectrometer in the reflection mode. The 355 nm line of violet diode laer with a spot size of 20 mm and a power of 10 mW was used as the excitation source. The diamond anvil cell (DAC) containing the sample was put on Nikon fluorescene microscope to focus the laser on the sample. Optical photographs of the compressed samples were obtained using an imaging camera (Canon EOS 5D Mark II) equipped on the fluorescence microscope.

Computational details.

Ab initio calculations were carried out with the Gaussian 09 program.[S1] Geometry at ground state was optimized with the density functional theory (DFT) using the B3LYP functional and 6–31G** basis set. The single point energy calculation was performed in the crystal state for **1OC** and **1RC**. The vertical excitations were performed with time-dependent density functional theory (TD-DFT) at the same level of theory by iteratively solving 20 states for **1OC** and **1RC**.

Single Crystal Structure

Single crystal X-ray diffraction data were collected on a Rigaku RAXIS-PRID diffractometer using the ω-scan mode with graphite-monochromator Mo Kα radiation. The structures were solved with direct methods using the SHELXTL programs and refined with full-matrix leastsquares on F^2. Non-hydrogen atoms were refined anisotropically. The positions of hydrogen atoms were calculated and refined isotropically. CCDC 1037296 and 1037297 contains the supplementary crystallographic data for this paper. These data can be obtained free of charge from The Cambridge Crystallographic Data Centre via www.ccdc.cam.ac.uk/data_request/cif.

S1 Gaussian 09, Revision D.01, M. J. Frisch, G. W. Trucks, H. B. Schlegel, G. E. Scuseria, M. A. Robb, J. R. Cheeseman, G. Scalmani, V. Barone, B. Mennucci, G. A. Petersson, H. Nakatsuji, M. Caricato, X. Li, H. P. Hratchian, A. F. Izmaylov, J. Bloino, G. Zheng, J. L. Sonnenberg, M. Hada, M. Ehara, K. Toyota, R. Fukuda, J. Hasegawa, M. Ishida, T. Nakajima, Y. Honda, O. Kitao, H. Nakai, T. Vreven, J. A. Montgomery, Jr., J. E. Peralta, F. Ogliaro, M. Bearpark, J. J. Heyd, E. Brothers, K. N. Kudin, V. N. Staroverov, R. Kobayashi, J. Normand, K. Raghavachari, A. Rendell, J. C. Burant, S. S. Iyengar, J. Tomasi, M. Cossi, N. Rega, J. M. Millam, M. Klene, J. E. Knox, J. B. Cross, V. Bakken, C. Adamo, J. Jaramillo, R. Gomperts, R. E. Stratmann, O. Yazyev, A. J. Austin, R. Cammi, C. Pomelli, J. W. Ochterski, R. L. Martin, K. Morokuma, V. G. Zakrzewski, G. A. Voth, P. Salvador, J. J. Dannenberg, S. Dapprich, A. D. Daniels, Ö. Farkas, J. B. Foresman, J. V. Ortiz, J. Cioslowski, and D. J. Fox, Gaussian, Inc., Wallingford CT, 2009.

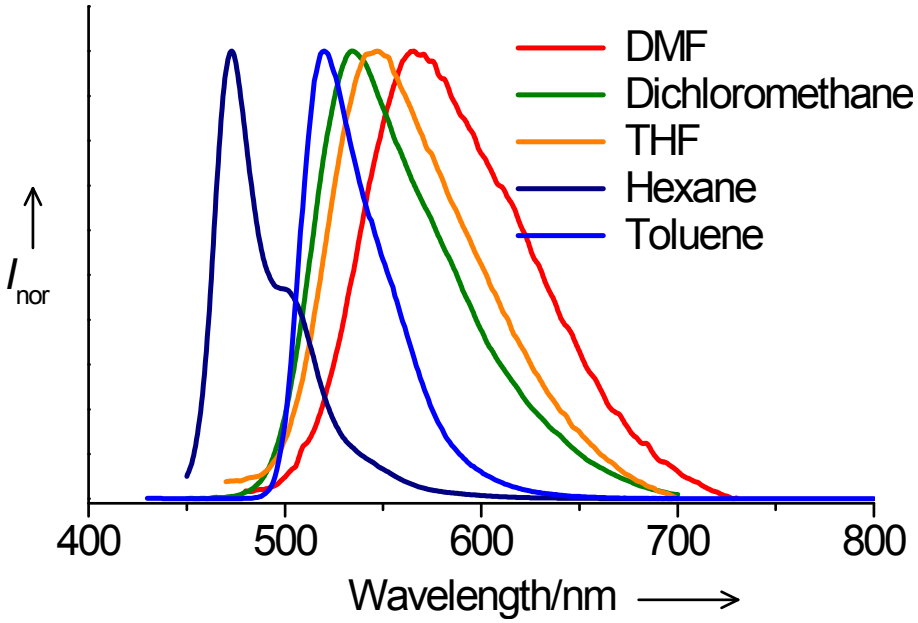

Figure S1 Solvent-dependent emission spectrum of compound **1**.

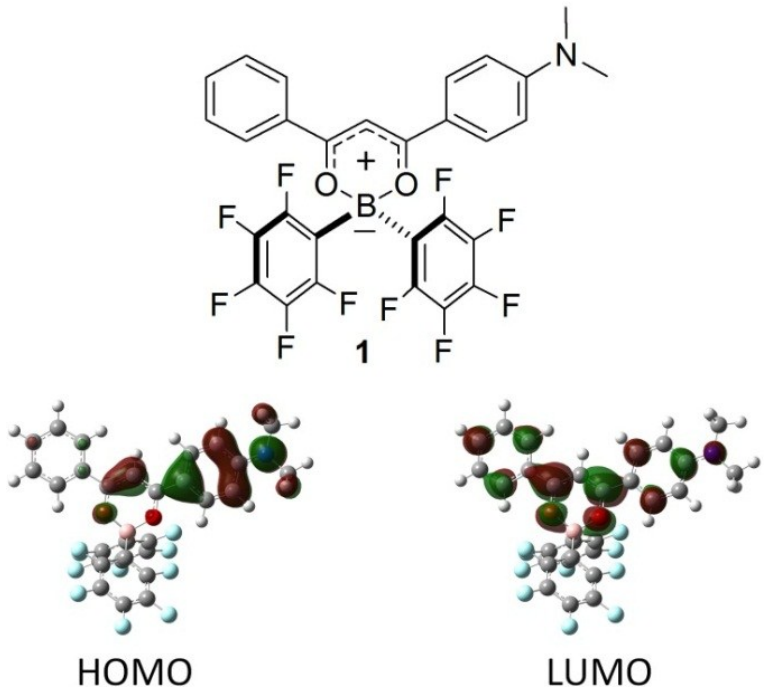

Figure S2. Chemical and electronic structures of compound **1**.

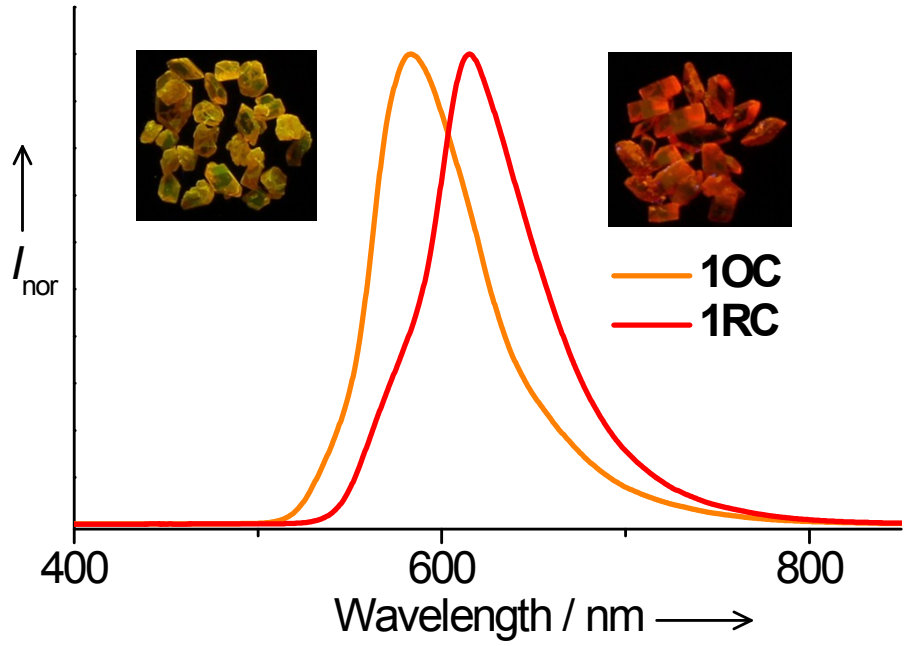

Figure S3 Emission spectra of crystalline samples **1OC** and **1RC**.

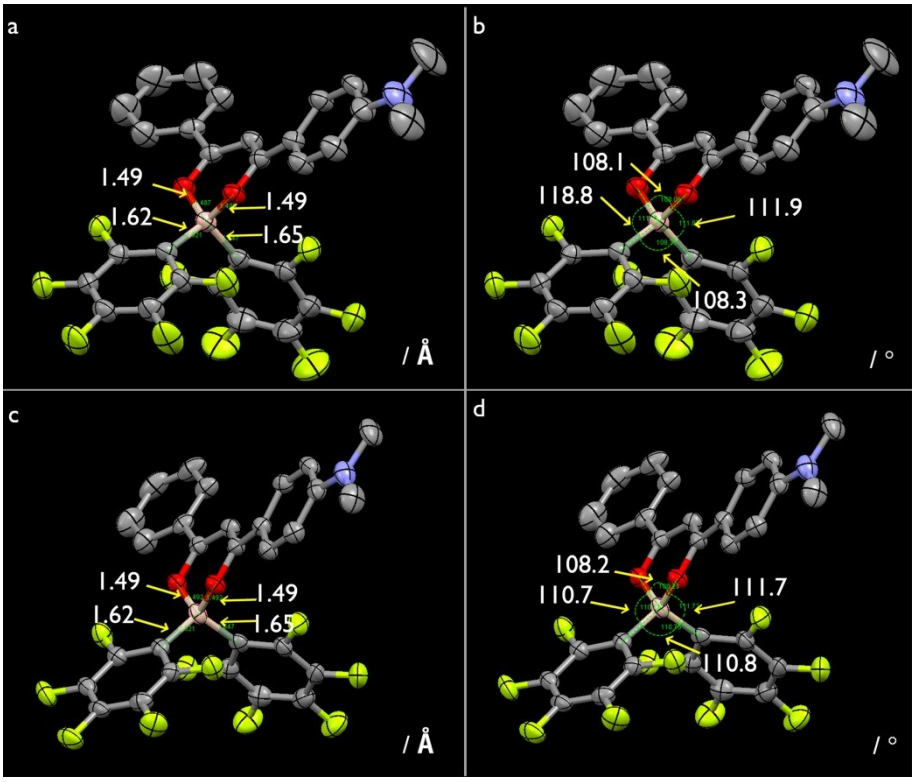

Figure S4. Selected bond angles and lenghts of crystals **1OC** and **1RC**.

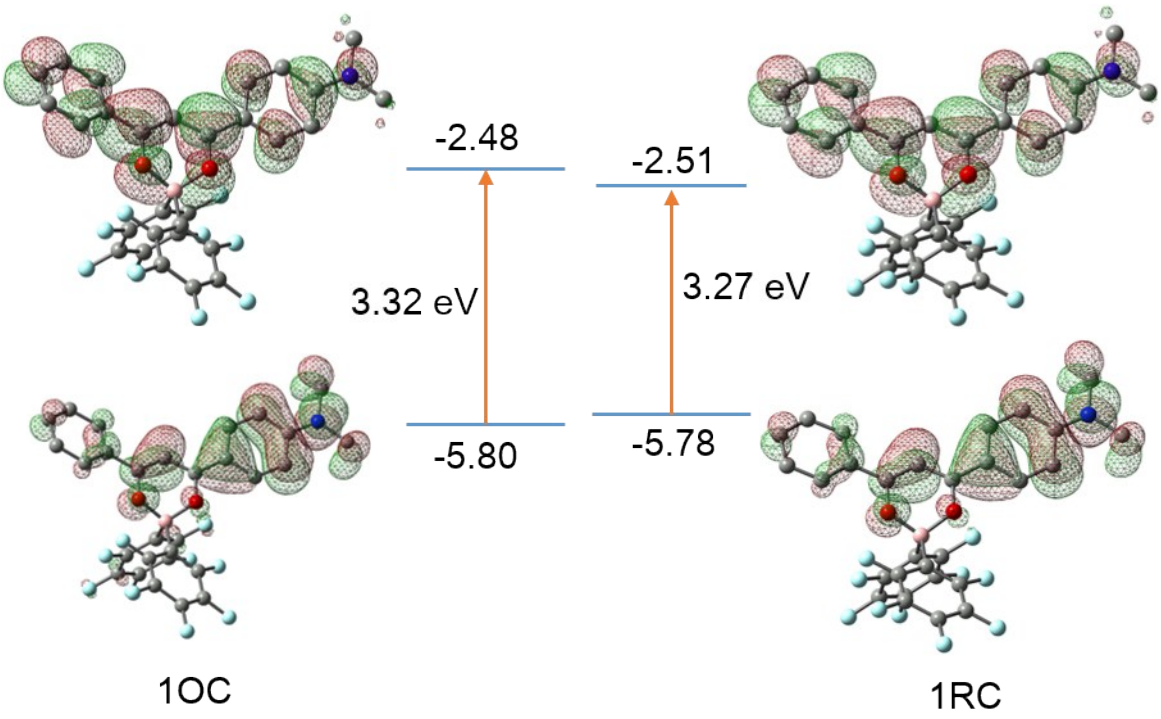

Figure S5. The calculated HOMOs and LUMOs as well as energy gaps for the two conformations **1OC** and **1RC**.

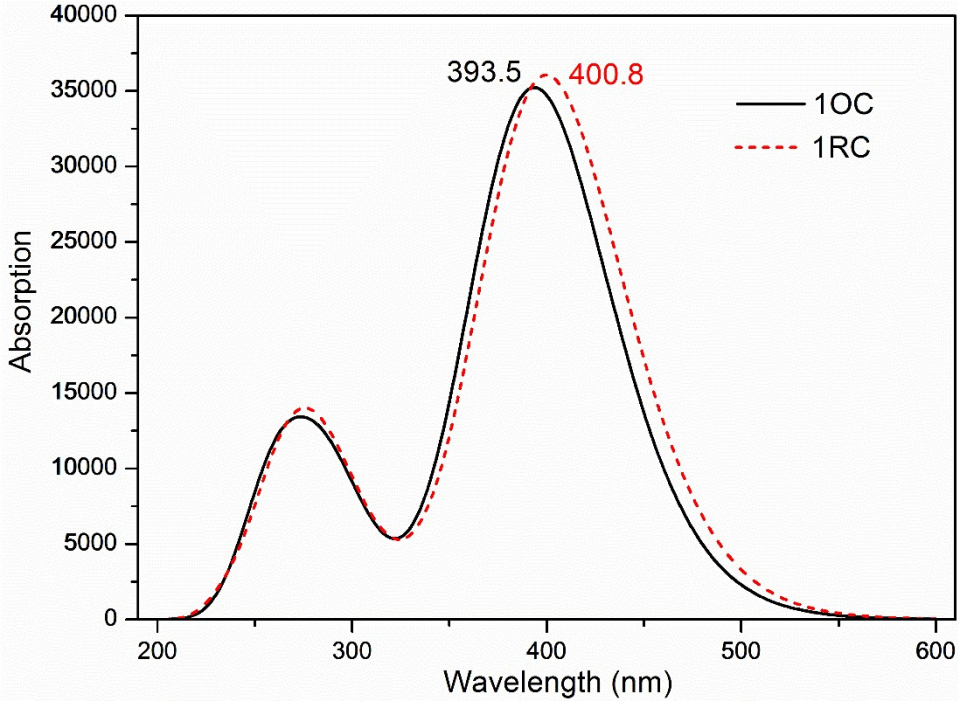

Figure S6. The simulated absorption spectra based on the two conformations observed in the crystal structures **1OC** and **1RC**.

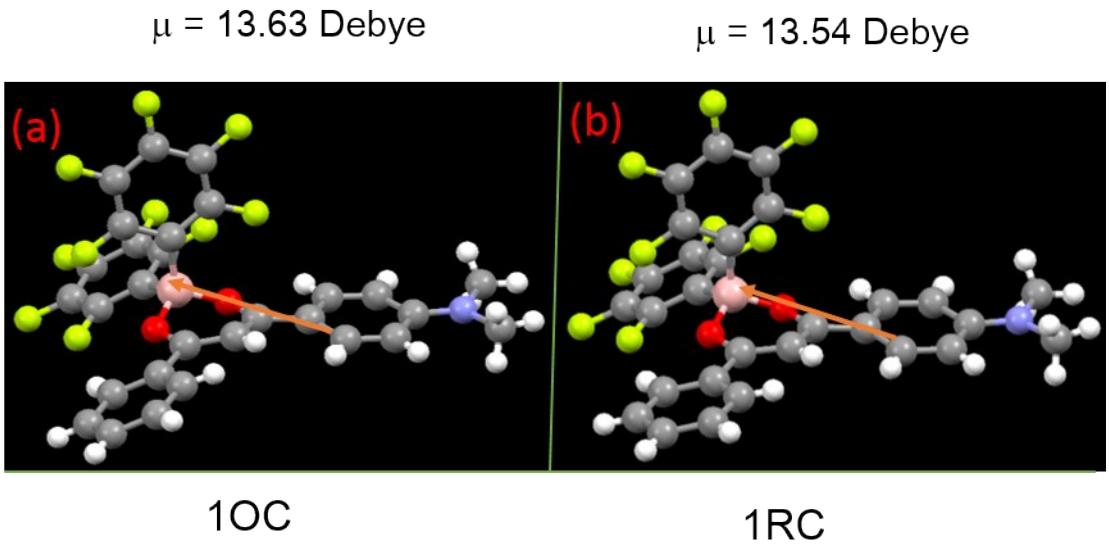

Figure S7. The calculated transition dipole moments in the crystal states for **1OC** and **1RC**.

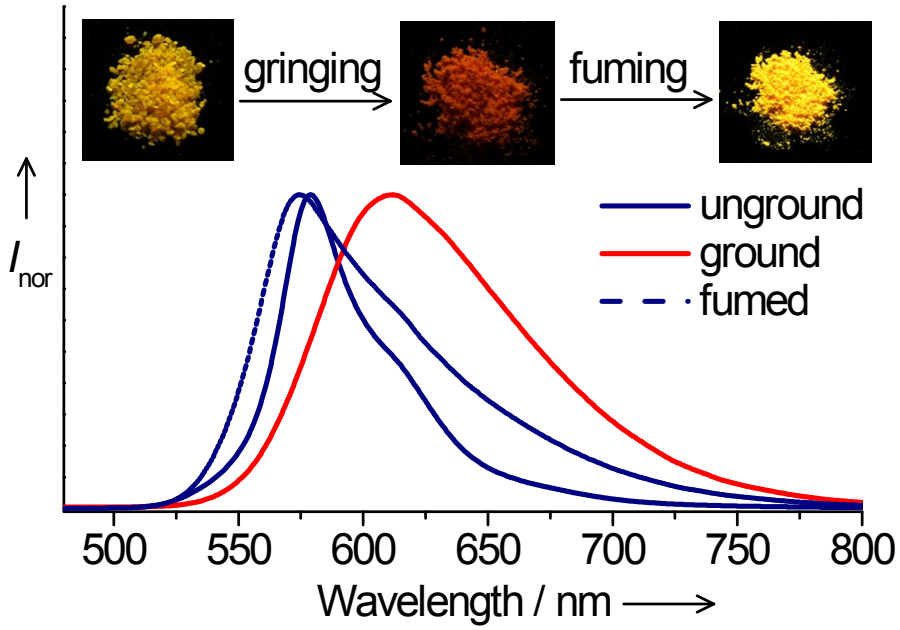

Figure S8 Emission spectra of ungrond, ground, and annealed sample of **1O**.

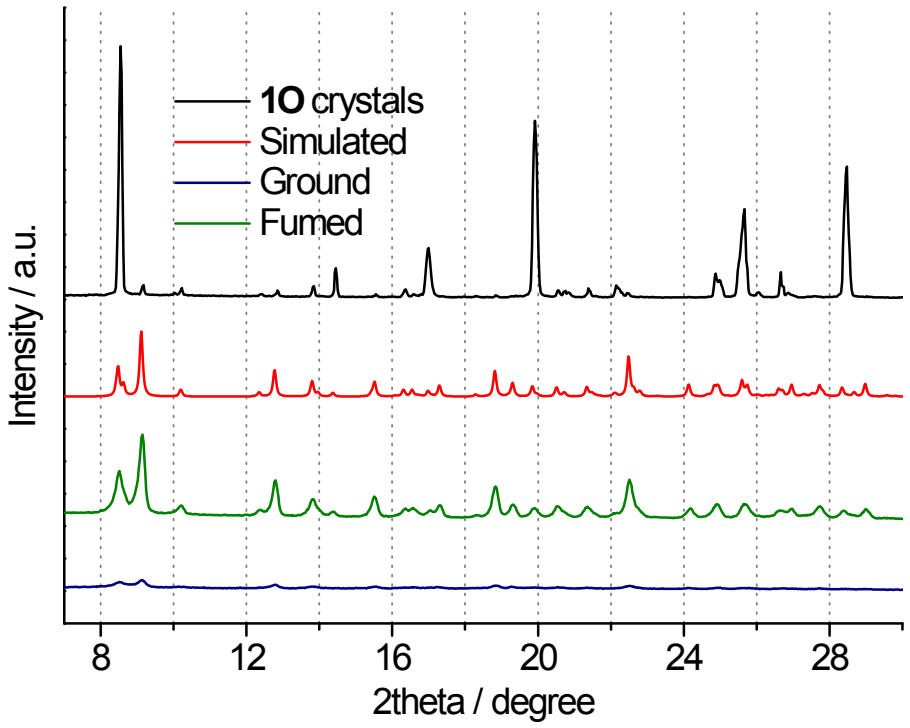

Figure S9. Powder X-ray diffraction curves of **1O** sample in various states.

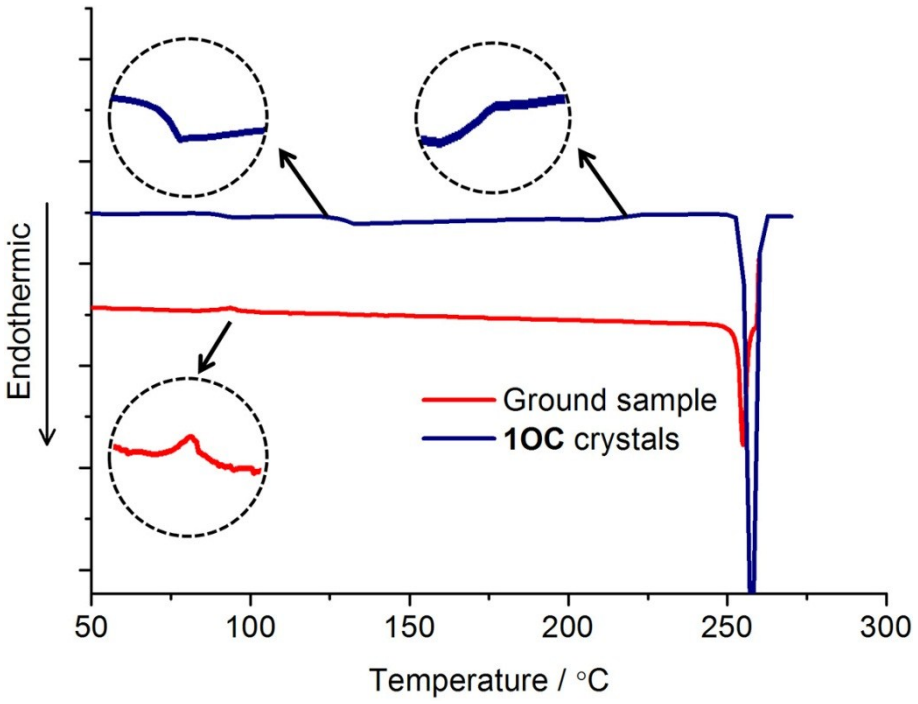

Figure S10 DSC curve of **1OC** bulk crystals and the ground sample.

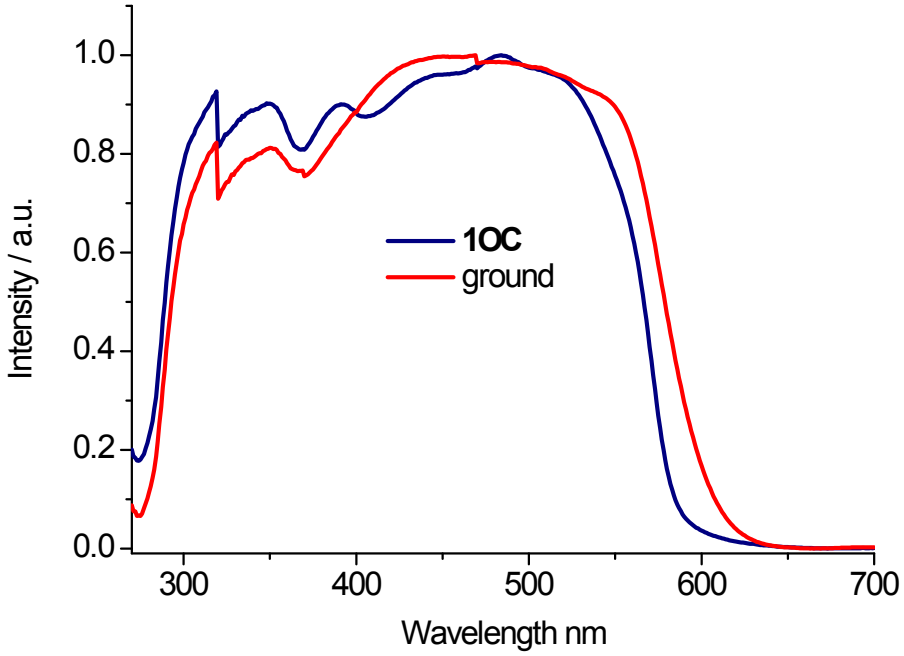

Figure S11. Absorption spectra of **1OC** crystals and ground sample.

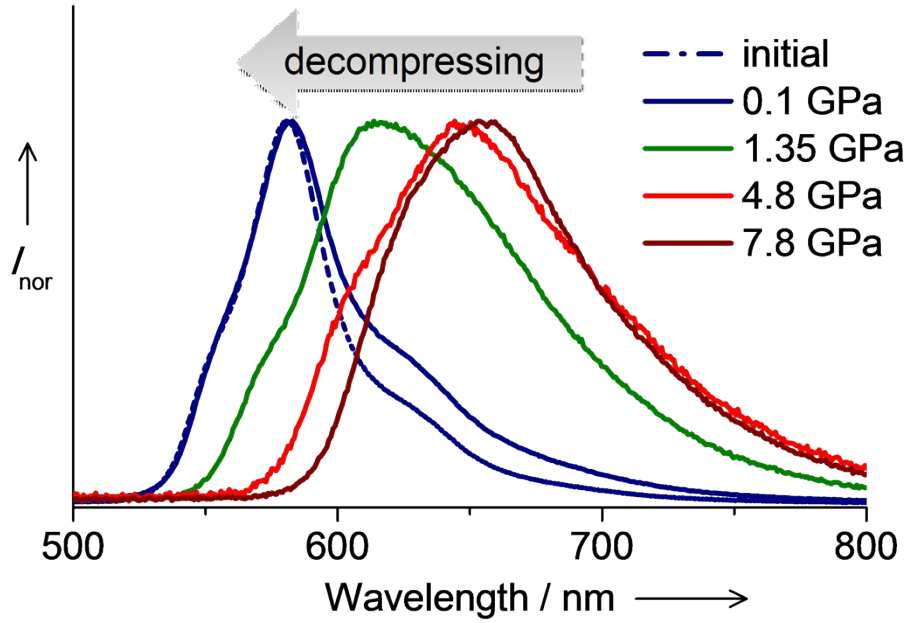

Figure S12. Emission spectra of crystal **1OC** recorded in the decompression process.

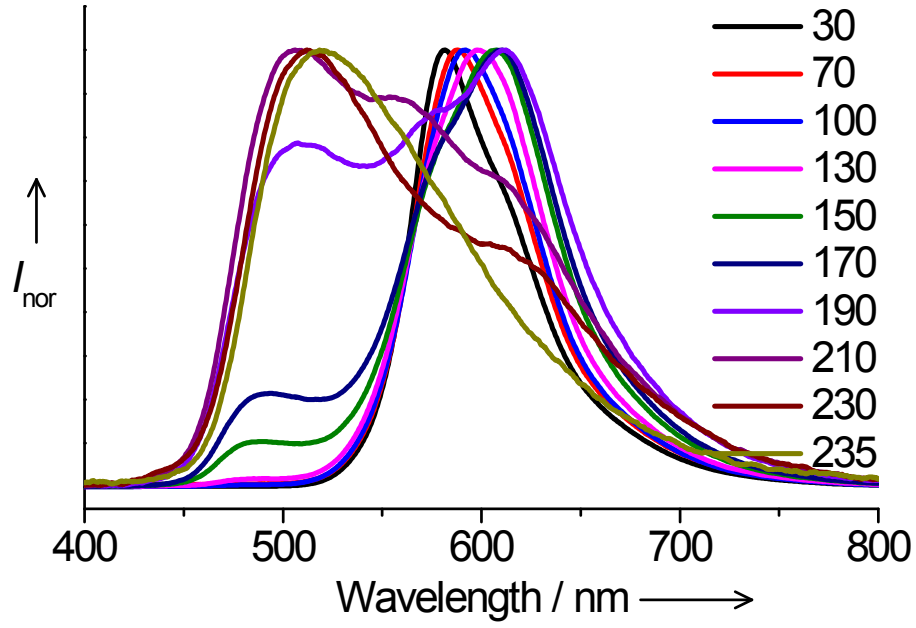

Figure S13 Temperature-dependent emission spectra of crystal **1OC**.

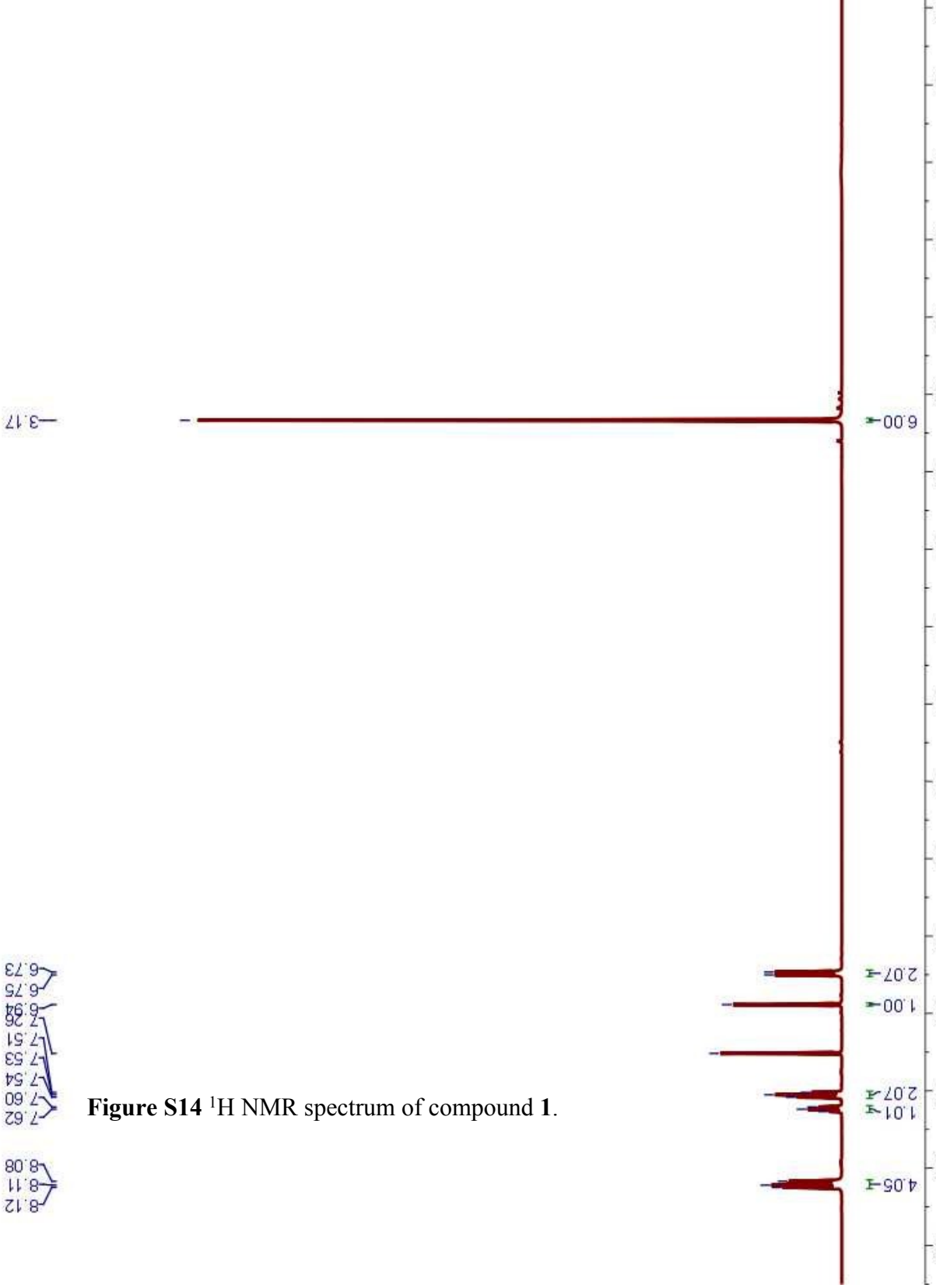

Figure S14 ^{1}H NMR spectrum of compound **1**.

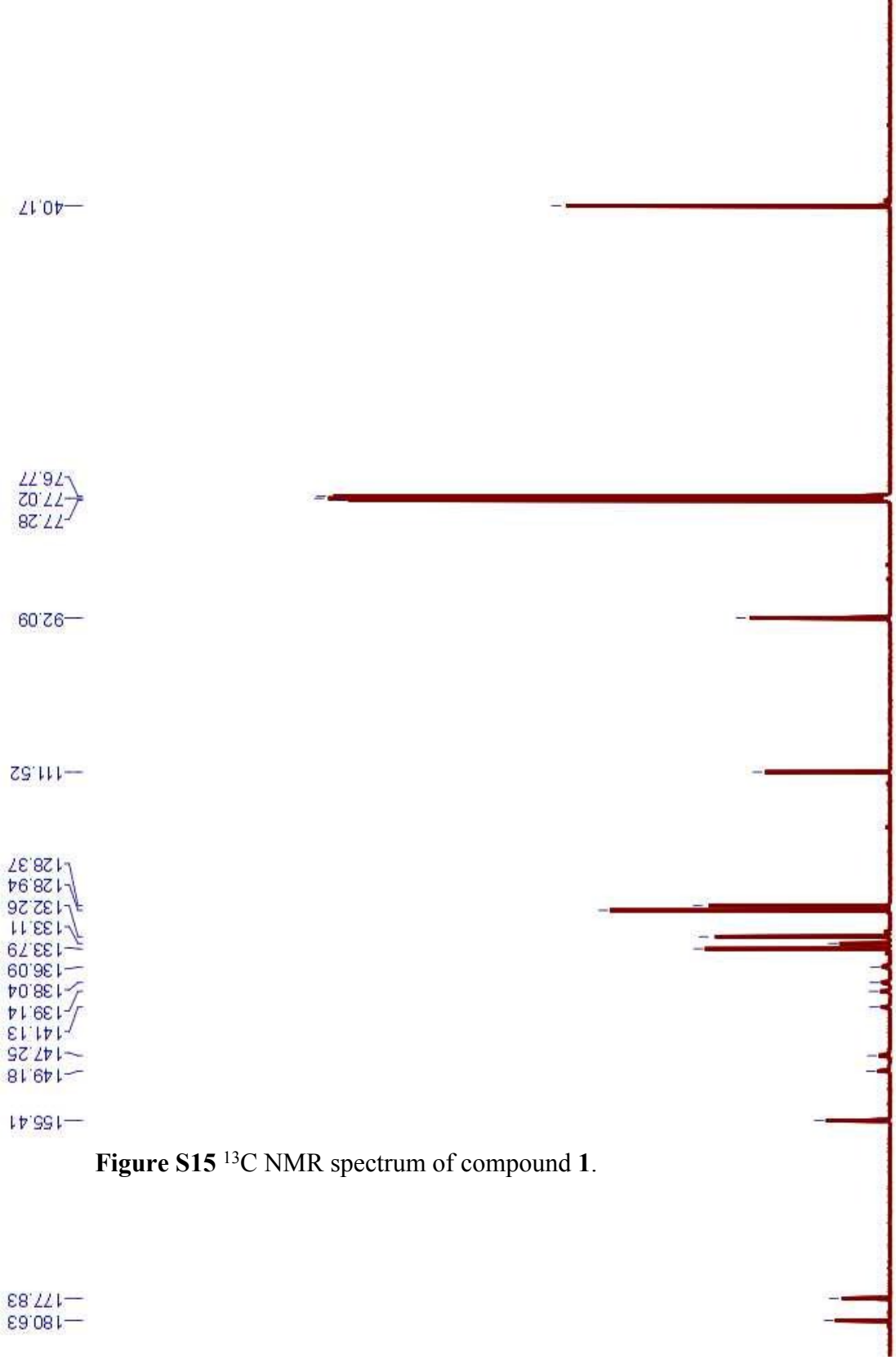

Figure S15 ^{13}C NMR spectrum of compound **1**.